

Suppressed epidemics in multi-relational networks

Elvis H. W. Xu,¹ Wei Wang,² C. Xu,³ Ming Tang,² Younghae Do,⁴ and P. M. Hui¹

¹*Department of Physics, The Chinese University of Hong Kong, Shatin, New Territories, Hong Kong SAR, China*

²*Web Sciences Center, University of Electronic Science and Technology of China, Chengdu 610054, China*

³*College of Physics, Optoelectronics and Energy, Soochow University, Suzhou 215006, China*

⁴*Department of Mathematics, Kyungpook National University, Daegu 702-701, South Korea*

(Dated: August 27, 2021)

A two-state epidemic model in networks with links mimicking two kinds of relationships between connected nodes is introduced. Links of weights w_1 and w_0 occur with probabilities p and $1 - p$, respectively. The fraction of infected nodes $\rho(p)$ shows a non-monotonic behavior, with ρ drops with p for small p and increases for large p . For small to moderate w_1/w_0 ratios, $\rho(p)$ exhibits a minimum that signifies an optimal suppression. For large w_1/w_0 ratios, the suppression leads to an absorbing phase consisting only of healthy nodes within a range $p_L \leq p \leq p_R$, and an active phase with mixed infected and healthy nodes for $p < p_L$ and $p > p_R$. A mean field theory that ignores spatial correlation is shown to give qualitative agreement and capture all the key features. A physical picture that emphasizes the intricate interplay between infections via w_0 links and within clusters formed by nodes carrying the w_1 links is presented. The absorbing state at large w_1/w_0 ratios results when the clusters are big enough to disrupt the spread via w_0 links and yet small enough to avoid an epidemic within the clusters. A theory that uses the possible local environments of a node as variables is formulated. The theory gives results in good agreement with simulation results, thereby showing the necessity of including longer spatial correlations.

PACS numbers: 89.75.Hc, 87.19.X-, 87.23.Ge

I. INTRODUCTION

The past 15 years have witnessed the rapid development in complex network science and its applications [1, 2]. Besides structural properties, how network topology, dynamical behavior and functionality are coupled together has been a focus of research and much work has been done within a single complex network [2–4]. Recent works have revealed that the heterogeneous nature of the nodes and links, often interpreted as multilayer networks, inter-dependent networks and interconnected networks, is crucial for understanding the properties of real-world complex systems such as social networks, complex infrastructures, and brain networks [5–10]. With a network with a specific function, e.g. for information flow, power grid, vehicular traffic, and air traffic, representing a layer, the proper functioning of an entire complex system is related to the simultaneous operation of an interacting set of networks. Recent studies along this line include empirical analysis of real-world network data [11, 12], evolution of network structures [13–15], and new critical phenomena and processes occurring on them [9, 10, 16, 17]. These coupled networks exhibit some common features, such as the inter-degree-degree correlation [18], inter-similarity [19], multiple dependence in providing support [9], and node and edge overlapping between layers [20]. These features have important effects on critical phenomena and the dynamics, including percolation [9], cascading failure [16], diffusion processes [21], emergence of cooperation [22] and epidemic dynamics [17], when compared with those in a single network. For example, Buldyrev *et al.* found that strong structural heterogeneity increases the vulnerability of multilayer networks to random failure, an effect opposite to that in a single network [16]. For spreading dynamics in layered networks,

Wang and coworkers found that the degree-degree correlation between the layered networks cannot change the information threshold, but make the system more resilient to epidemic outbreak [23].

In the present work, we focus on multi-relational networks. The simplest form of it refers to a set of nodes that are connected by two or more types of links, signifying links of different importance or relationships. They can also be regarded as a type of multilayer networks, with the same set of nodes connected differently in each layer representing, for example, different social relationships [8]. The relationships could be friends, relatives, colleagues, clients, and schoolmates, among others, in the context of a social network [24]; or enemies, guild members, and friends in online games [11]. The same cities on a map could be connected by different links representing highways, railways and airline routes [25]. The different links undoubtedly play different roles in spreading dynamics. Our everyday experience is that we would be selective in sharing our views or our latest updates, and would not share them equally with everyone we know. Often, individuals are more willing to share good news with their friends [26]. Two friends could communicate via several ways. The means of communication often reflects the urgency of the contents and phone calls are preferred over short messages in conveying urgent information to friends [27].

In epidemics, the chance of infecting another person is not even among all the ones that an infected person comes into contact. Instead, an infected person will have a higher chance of infecting another person who is in closer and longer contact, e.g. a colleague in the same office. The different importance among the links in a network with multi-relations gives rise to an uneven or biased chance of someone being infected. Here, we aim to study the effects of this biased se-

lection on the spreading dynamics. We propose and study a model that captures the non-trivial effects of two different kinds of links in a random regular network of degree k . A fraction p of the links carry a higher weight w_1 and the remaining $1 - p$ carry a weight w_0 . A link of higher weight has a higher chance to be used as a path for infection [28–30]. Within the susceptible-infected-susceptible (SIS) model of epidemics [31–34], we study the extent of an epidemic as measured by the fraction of infected sites ρ in the steady state as a function of p and the contrast w_1/w_0 in the weights in detail. It is found that $\rho(p)$ exhibits a non-monotonic dependence, with ρ drops with p for small p and increases for large p . For small to moderate w_1/w_0 ratios, ρ exhibits a minimum at some value of p . For large w_1/w_0 ratios, there exists a range of p in which the system carries 100% healthy nodes. This leads to a re-entrance behavior in which the system starts with an active and mixed phase consisting of both infected and healthy nodes for $0 \leq p \leq p_L$, makes a transition into an absorbing and all-healthy phase at $p = p_L$ and stays as such within a range $p_L \leq p \leq p_R$, and re-enters into an active and mixed phase for $p_R < p < 1$. To understand the behavior, we report results of two analytic approaches together with a physical picture. We set up a single-site mean field approach that captures all these features. Despite the theory only gives qualitative agreement with simulation results, it has the merit that analytic expressions for $\rho(p)$ in the $p \rightarrow 0$ and $p \rightarrow 1$ limits can be derived. It also gives phase diagram that exhibits the re-entrance behavior when the contrast w_1/w_0 is above a threshold. A physical picture that emphasizes the importance of the clusters formed by nodes that carry links with the higher weight then emerges. These links serve to confine the spread. At small p , the cluster sizes are small and disease in such small clusters cannot sustain. Thereby, they serve as sinks for the disease and effectively reduce the infection probability and lead to a drop in ρ . At large p , there is a big cluster and the disease can be sustained within the cluster. Replacing some w_1 links by w_0 links reduces effectively the infection probability and ρ drops from the $p = 1$ limit. For sufficiently large w_1/w_0 , 100% healthy phase is achieved for a range of p when the cluster sizes are big enough to disrupt the spread via w_0 links and yet not so big for the disease to sustain through infections in the clusters. We further constructed a more accurate theory that uses the different local environments of a node as the variables [35]. The theory, with its longer spatial correlation, is shown to give results in quantitative agreement with simulation results.

The plan of the paper is as follows. In Sec. II, the model of spreading dynamics in a network with links corresponding to two kinds of relationship is defined. Key features of $\rho(p)$ on other parameters of the model as observed in detailed numerical simulations are described in Sec. III. In Sec. IV, we develop a mean-field theory and show that the theory exhibits all the observed features, although the agreement is only quantitative. A phase diagram that exhibits the re-entrance behavior is constructed. A physical picture on the role of the inhomogeneity among the links is presented. In Sec. V, we describe the construction of an improved theory based on considering the dynamics of the local environment of a node. The theory

is shown to give good agreement with simulation results. We summarize the work in Sec. VI.

II. MODEL

Consider a network consisting of N nodes. A node i is connected to k_i other nodes. Each link that connects two nodes i and j in the network carries a weight w_{ij} , which is assigned when the network is constructed and its value remains unchanged. The different weights among the links represent different kinds of relationship. Within the context of an epidemic model, each node, representing a person, can be in one of two states: susceptible (S) or infected (I). We study the effects of inhomogeneous weighting of the links on a SIS epidemic model, based on a contact process [36–38]. In a time step, every infected node i selects one of the k_i neighbors, say node j , for a possible infection with the probability

$$\mathcal{P}_{ij} = \frac{w_{ij}}{\sum_{j \in \{i\}} w_{ij}}, \quad (1)$$

where the summation in the denominator is over the set $\{i\}$ of k_i nodes that are connected to the node i . The selection is thus biased by the weights of the links. If the selected neighbor is in the susceptible state S , then it will be infected with an infection probability λ . Once infected, its state becomes I . If the selected neighbor is already in the infected state I , then it will remain in state I . A recovery process is then carried out in which every infected node at the beginning of the time step would recover to become state S with a recovery probability γ . The epidemic dynamics is then repeated. A quantity of interest is the fraction of infected nodes in the system in the steady state. Note that for a realization of the network, \mathcal{P}_{ij} is a property of a link and it does not evolve in time.

To study how the coexistence of links of different weights affects the extent of an epidemic, we consider a distribution $\mathcal{D}(w_{ij})$ in the weights among the links of the form

$$\mathcal{D}(w_{ij}) = (1 - p) \delta(w_{ij} - w_0) + p \delta(w_{ij} - w_1). \quad (2)$$

It represents a system with two types of relationship. The network has a fraction $1 - p$ of the links carrying a weight of w_0 and a fraction p carrying a weight of w_1 . A few points should be noted from the expression of \mathcal{P}_{ij} for a realization of the weighted network. The weights w_0 and w_1 are used in preferentially selecting a neighbor and it is the ratio $w = w_1/w_0$ that matters. The cases in which a network consisting only of a single type of links, i.e., w_0 links ($p = 0$), w_1 links ($p = 1$), and $w_0 = w_1$ (all values of p), are equivalent.

In numerical simulations, there are different sources of randomness. Even for a given degree distribution for the nodes, the connections among the N nodes vary in different realizations. In addition, the assignment of w_0 and w_1 to the links can also be different between realizations for a given value of p , even if the links are fixed in a network. In what follows, results from simulations are obtained by averaging over 100 different realizations of network construction and weight assignment. The initial condition is that of a whole lattice of

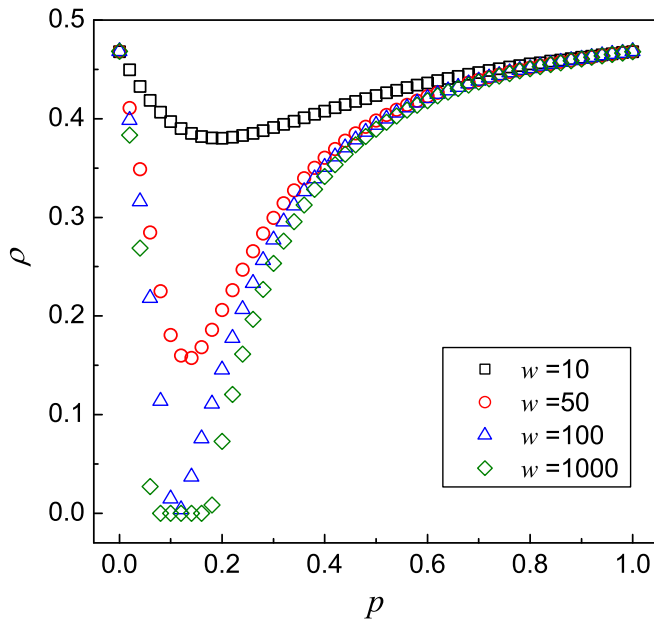


FIG. 1: The fraction of infected nodes ρ as a function of the fraction p of heavier weighted links. Results are obtained by numerical simulations in random regular networks of degree $k = 10$. The SIS model parameters are $\lambda = 0.02$ and $\gamma = 0.01$. Results for links with a weight ratio $w = w_1/w_0 = 10, 50, 100$ and 1000 are shown by different symbols with $w_0 = 1$.

infected nodes and results are recorded after the system has evolved beyond the transient period. Without loss of generality, we set $w_0 = 1$ and vary w_1 for $w_1 > 1$. Thus $w > 1$. The averaged fraction of infected nodes is denoted by ρ , which is a function of p , λ , and γ . In defining the problem, we intentionally allow for the possibility of studying different types of networks as given by a distribution in the degrees k_i and different types of weight distribution $\mathcal{D}(w_{ij})$.

III. KEY FEATURES IN SIMULATION RESULTS

For concreteness, we focus on implementing the model in random regular networks with nodes all having the same degree k . Figure 1 shows the dependence of ρ on the fraction of weighted links p for different values of $w = w_1/w_0$ in networks with $N = 5000$ nodes and $k = 10$. The SIS model parameters are $\lambda = 0.02$ and $\gamma = 0.01$. The equivalence of the $p = 0$ and $p = 1$ cases necessarily leads to a non-monotonic behavior of $\rho(p)$. For a ratio of $w = 10$, the results are typical with the key features that (i) a dilute fraction of heavier weighted links suppresses ρ , (ii) $\rho(p)$ increases with p for a wide range of larger values of p , and (iii) there is a value of p at which ρ is a minimum. These general features remain for higher w_1/w_0 contrast, as shown in the results for $w_1/w_0 = 50$ and 100 in Fig. 1.

For $w_1/w_0 \gg 1$, e.g. $w_1/w_0 = 1,000$ (see Fig. 1), a re-entrance behavior is observed. The drop in $\rho(p)$ for small p is so strong that ρ vanishes at a value of $p = p_L$. For a range

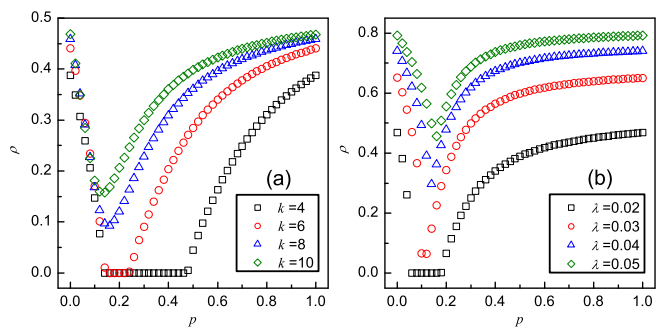


FIG. 2: The fraction of infected nodes ρ as a function of the fraction p of heavier weighted links as obtained by numerical simulations. (a) Results in random regular networks of different degrees $k = 10, 8, 6,$ and 4 . The SIS model parameters are $\lambda = 0.02$ and $\gamma = 0.01$. The ratio of the weights in the links is $w_1/w_0 = 50$. (b) Results for different values of the infection probability $\lambda = 0.02, 0.03, 0.04$ and 0.05 in random regular networks of $k = 10$. The ratio of the weights in the links is $w_1/w_0 = 10,000$, and the recovery probability is $\gamma = 0.01$.

$p_L \leq p \leq p_R$, $\rho = 0$ indicating the system evolves to a state with all nodes recovered and remain healthy. This corresponds to an absorbing phase in which the epidemic dynamics stops. The range of p with $\rho = 0$ widens for higher contrast w . Only for $p > p_R$ that a resulting state of $\rho \neq 0$ with finite infection re-emerges. The values of p_L and p_R are also dependent on the network parameters k and p and the SIS epidemic parameters λ and γ .

Figure 2 shows the dependence of ρ on the other parameters of the model. Figure 2(a) shows the behavior of $\rho(p)$ for different values of the degree k in the network structure, for fixed $w_1/w_0 = 50$, $\lambda = 0.02$ and $\gamma = 0.01$. For small p , $\rho(p)$ shows only a weak dependence on k before reaching its minimum. A larger degree suppresses the re-entrance behavior. As the degree of the network drops, the minimum in $\rho(p)$ goes deeper and the value of p at which the minimum occurs shifts higher. As the degree becomes sufficiently small, the drop in ρ at small p is more pronounced so that $\rho = 0$ for $p > p_L$ for $k = 6$ and $k = 4$. The range of p between p_R and p_L increases as k decreases. For larger values of p , a network of a higher degree gives a higher infected fraction. Figure 2(b) shows the behavior of $\rho(p)$ for different values of the infection probability λ in networks with $k = 10$, $w_1/w_0 = 10,000$ and $\gamma = 0.01$. The infected fraction is generally higher for a higher infection probability. For cases in which there exists a range of p with $\rho = 0$ for a smaller value of λ (see for example $\lambda = 0.02$), an increased λ will lift $\rho(p)$ up to the extent that the $\rho = 0$ state does not exist anymore.

IV. QUALITATIVE TREATMENT, PHASE DIAGRAM AND PHYSICAL PICTURE

A mean field treatment that gives qualitative agreement with simulation results and captures all the key features can be formulated readily. We ignore any spatial correlation gen-

erated by the infection process and assume that the infected nodes at a moment in time are randomly distributed on the random regular network. Together with the fact that the weighted links are randomly assigned, the probability that an infected node chooses a susceptible neighbor for a possibility infection via a link of weight w_0 is given according to Eq. (1) by

$$\mathcal{P}_{w_0} = \frac{1}{1 + (k-1)(1-p) + (k-1)pw}, \quad (3)$$

where w is the ratio of the two weights. Similarly, the probability that an infected node chooses a susceptible neighbor for a possibility infection via a link of weight w_1 is

$$\mathcal{P}_{w_1} = \frac{w}{(k-1)(1-p) + w + (k-1)pw}. \quad (4)$$

A dynamical equation for the density of infected nodes ρ can then be written down as

$$\frac{d\rho}{dt} = (1-\rho)\lambda \cdot k\rho [(1-p)\mathcal{P}_{w_0} + p\mathcal{P}_{w_1}] - \gamma\rho, \quad (5)$$

where the first term on the right-hand-side of Eq. (5) describes the changes in ρ due to the infection and the second term accounts for recovery.

Solving $d\rho/dt = 0$ for the density of infected nodes in the steady state $\rho^{(MF)}$ within the mean field theory gives

$$\rho^{(MF)} = 1 - \frac{1}{k((1-p)\mathcal{P}_{w_0} + p\mathcal{P}_{w_1})} \frac{\gamma}{\lambda}. \quad (6)$$

For the cases of $p = 0$ and $p = 1$, $\mathcal{P}_{w_0} = \mathcal{P}_{w_1} = 1/k$ and thus $\rho^{(MF)}(p = 0) = \rho^{(MF)}(p = 1)$ as required. However, the value $\rho^{(MF)}(p = 0) = \rho^{(MF)}(p = 1) = 1 - \gamma/\lambda$, which is the result of a random regular network, is slightly higher than the simulation results and it does not show a k -dependence as observed numerically. Despite the agreement is only qualitative, the solution captures all the key features as we now discuss. The solution in Eq. (6) has a factor in front of γ/λ that provides the dependence on k and $w = w_1/w_0$ for $0 < p < 1$. For given k and w , Eq. (6) gives

$$\rho^{(MF)} \approx 1 - \frac{\gamma}{\lambda} \left(1 + \frac{(k-1)(w-1)^2}{k(k-1+w)} p \right) \quad (7)$$

in the limit of $p \rightarrow 0$. This shows explicitly a drop in ρ_s from its value of $1 - \gamma/\lambda$ at $p = 0$ as p increases. Similarly, Eq. (6) gives

$$\rho^{(MF)} \approx 1 - \frac{\gamma}{\lambda} \left(1 + \frac{(k-1)(w-1)^2}{kw(1+(k-1)w)} q \right) \quad (8)$$

with $q = 1-p \rightarrow 0$ in the $p \rightarrow 1$ limit and predicts an increase towards the value of ρ at $p = 1$ as $p \rightarrow 1$. Both features are in agreement with simulation data.

The theory also predicts the existence of a minimum of ρ , as well as a range of p in which $\rho = 0$ under suitable conditions and thus the re-entrance behavior. As \mathcal{P}_{w_0} and \mathcal{P}_{w_1} also depend on p , setting $\rho^{(MF)} = 0$ in Eq. (6) gives a quadratic equation for p with the solutions

$$p_L = \frac{\gamma - \frac{2k(\lambda-\gamma)}{w-1} - \sqrt{\gamma^2 - \frac{4k^2 w \lambda (\lambda-\gamma)}{(k-1)(w-1)^2}}}{2(k\lambda - (k-1)\gamma)}, \quad (9)$$

$$p_R = \frac{\gamma - \frac{2k(\lambda-\gamma)}{w-1} + \sqrt{\gamma^2 - \frac{4k^2 w \lambda (\lambda-\gamma)}{(k-1)(w-1)^2}}}{2(k\lambda - (k-1)\gamma)}. \quad (10)$$

The values p_L and p_R , which depend on the network structural parameters k and w as well as the SIS parameters λ and γ , may take on complex values. In this case, the theory predicts that $\rho > 0$ over *all* values of p with a minimum at some value of p . The system thus remains in an active phase, i.e., the epidemic dynamics never stops. An alternative interpretation of the result is that for the whole range of p , the given infection probability λ is above the infection threshold determined by the network structural parameters and recovery probability and thus leading to $\rho \neq 0$. Under suitable conditions, p_L and p_R are real and the two values separate three different regimes. For $p < p_L$ and $p > p_R$, the system reaches an active and mixed phase with coexisting susceptible and infected nodes. For $p_L \leq p \leq p_R$, the system evolves into an absorbing and healthy phase ($\rho = 0$) with all the nodes being susceptible nodes, i.e., an AIIIS phase. Alternatively, the infection probability is below the corresponding threshold. All these features are in agreement with simulation data. As discussed in Fig. 1 and Fig. 2, the healthy phase and the associated re-entrance behavior emerge when w is sufficiently large, for given k , γ and λ . Using Eq. (9) or Eq. (10), p_L and p_R will take on real values for $w > w_c$, where the critical value w_c is given by

$$w_c = 1 + \frac{2((k^2\lambda^2 + \Phi) - k^2\lambda\gamma)}{\gamma^2(k-1)}, \quad (11)$$

where $\Phi = \sqrt{k^2(\gamma - \lambda)\lambda(k^2\lambda\gamma(1 - \lambda) - \gamma^2(k-1))}$.

With a theory capable of exhibiting all the key features, it will be a convenient tool for exploring the existence of different phases in the parameter space. As an example, Fig. 3(a) shows the possible phases in the p - w parameter space related to the network structure, for fixed values of $k = 10$, $\lambda = 0.02$ and $\gamma = 0.01$. In this case, $w_c \approx 90.88$ as indicated by the horizontal dashed line. For $w < w_c$ (see Region (I)), the system is in an active and mixed phase labelled by S+I over the whole range of p . This is the region in which ρ remains finite for all values of p and shows a minimum. For $w > w_c$, there are two phase boundaries as given by Eq. (9) (see thinner line on the left) and Eq. (10) (see thicker line on the right). In between these phase boundaries is a region (see Region (III)) in which the system evolves into a phase with only susceptible nodes (labelled AIIIS). On either side of the AIIIS region are regions corresponding to the active and mixed phase (labelled S+I) for small p (see Region (II)) and large p (see Region (IV)).

A physical picture on the effects of an inhomogeneous link weighting emerges from detailed analysis of simulation data and the mean field approach. It will be convenient for later discussions to regard the network as consisting of three components: two types of clusters connected by bridge links, as shown in Fig. 4(a). Here, the thin (thick) lines are links of weight w_0 (w_1), and the open and closed circles are S and I nodes, respectively. Nodes with *all* the links having the smaller weight w_0 are called A-type nodes. Nodes with *one or more* links of the higher weight w_1 are called B-type nodes.

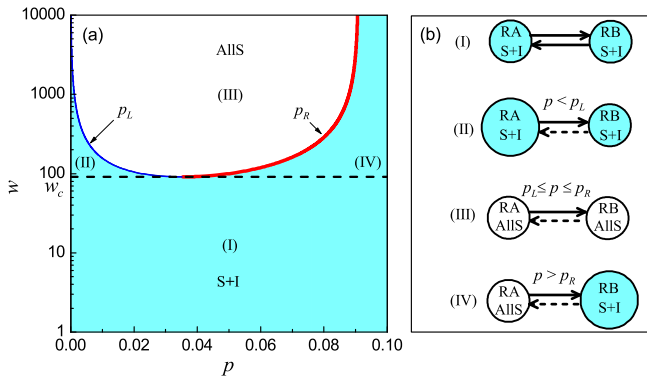


FIG. 3: (color online) (a) Phase diagram plotted in p - w space for $k = 10$, $\lambda = 0.02$ and $\gamma = 0.01$, showing four regions (I), (II), (III), (IV) of different qualitative behavior. The phase boundaries (thinner blue line and thicker red line) that separates the healthy (AIIIS) phase and a mixed epidemic (S+I) phase (colored) are plotted using Eqs. (9) and (10). A threshold w_c (dashed line) marks two different behaviors. For $w < w_c$, the system is in a mixed phase for all values of p (region I). For $w > w_c$, the system shows a re-entrance behavior as a function of p , starting from a mixed phase (region II) at small p through a healthy phase (region III) for $p_L < p < p_R$ to a mixed phase (region IV) again for $p > p_R$. (b) Schematic diagrams showing the different mechanisms in spreading in the four regions in the phase diagram, as explained in the text.

An A-cluster is one that consists of A-type nodes linked together via links of weight w_0 , as shown in Fig. 4(b). Similarly, a B-cluster is one that consists of B-type nodes connected together. In the case of $w = w_1/w_0 \gg 1$, the weighted links w_1 play an important role as the disease would be trapped among the weighted links once it gets into a B-cluster. Figure 4(c), therefore, shows a B-cluster with the w_0 links removed. By definition, the links that connect a A-cluster and a B-cluster must be of weight w_0 . These links are important in understanding the physics in the model and they are called bridge-links. The part of the network shown in Fig. 4(a) consists of the A-cluster in Fig. 4(b) and the B-cluster in Fig. 4(c) connected by two bridge-links.

This picture of the network facilitates a qualitative understanding of the different regions in the phase diagram (see Fig. 3(a)). According to Eq. (1), once the disease reaches the nodes in a B-cluster, the weighted links w_1 will be preferentially selected for spreading the disease. Although the B-clusters do not absorb disease into them, as the bridge-links are of weight w_0 , they tend to retain the disease and this effect is increasingly important as w_1/w_0 increases. Consider Regions (II), (III), (IV) for $w > w_c$ for $w_1/w_0 \gg 1$. In Region (II) with $p < p_L$, there is a dilute fraction of heavily weighted w_1 links, forming B-clusters of small sizes. It should be noted that the SIS model in a sparse cluster either small in size or having a small degree, would evolve into a state with all susceptible (AIIIS) nodes, as readily seen in the extreme case of a two-node cluster in which the disease ends when one or two infected nodes recover. When a few of the $w_1 \gg w_0$ links are introduced, the network structure can be viewed as a big

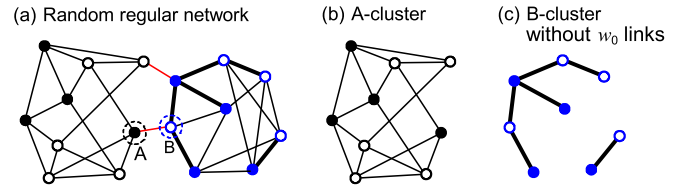


FIG. 4: (color online) (a) A sketch of a random regular network. The open (closed) circles represent nodes of state S (state I). Links of weight w_0 (w_1) are shown by the thinner (thicker) lines. Examples of an A-type nodes (marked A) carrying only w_0 links and a B-type node carrying has at least one w_1 link (marked B) are shown. Bridge-links that connect A-type and B-type nodes are of weight w_0 (thin red lines). (b) The A-cluster consisting of A-type nodes and w_0 links. (c) The B-cluster consisting of B-type nodes, but shown here with the w_0 links removed to emphasize the importance of the weighted links when $w = w_1/w_0 \gg 1$.

A-cluster in which isolated B-clusters of small sizes are embedded. The disease is sustained in the A-cluster, while once the disease gets into the B-cluster, the B-type nodes will not infect the neighboring A-type nodes again. If the B-clusters are isolated from the background A-cluster, the disease would die out within the B-cluster. However, the bridge-links continues to infect the B-type nodes that are connected to the A-cluster. Therefore, the B-cluster serves as a sink to the disease, as the disease could only get in but not out. This process is schematically shown in Fig. 3(b) for Region (II), with the thick and dashed arrows showing the asymmetry that A-type nodes would infect B-type nodes more readily than the other way round, while the big A-cluster is in a mixed phase and the B-type nodes at the bridge-links have the chance of being repeatedly infected making the small B-clusters also in a mixed phase (filled circles). Effectively, the presence of the B-clusters serve to reduce the tendency of spreading the disease by the A-type nodes. Mathematically, it is represented by an effective infection probability that is reduced from λ by a factor given by the terms in the parentheses in Eq. (7), leading to a drop in ρ . In Region (III) with $p_L \leq p \leq p_R$, the B-clusters grow in size but they are not big enough to support an epidemic within them. They continue to be sinks for the disease. However, the higher fraction of w_1 links are sufficient to reduce the size and the average degree of the A-clusters to the extent that the disease can no longer sustain. Without the continual infection via the bridge-links, the A-clusters and B-clusters eventually reach an AIIIS phase. This is schematically shown in Fig. 3(b) (Region III) with the open circles representing the AIIIS phase in the A-clusters and B-clusters. The arrows again represent the asymmetry in infection between A-clusters and B-clusters. In Region (IV) with $p > p_L$, the B-clusters are sufficiently large to sustain the epidemic within them. The effects that the B-clusters are sinks and the A-clusters get smaller as p increases put the A-clusters in an AIIIS phase. As p increases, the number of healthy A-nodes drops and ρ increases. The epidemic thus proceeds and sustains only within the B-clusters. The A-clusters disappear well before the $p \rightarrow 1$ limit because a dilute fraction of w_0 links is

insufficient to form A-clusters. As $p \rightarrow 1$, the network structure is that of a big B-cluster in which there are some isolated links of weight w_0 . These isolated links have the effect of reducing the number of neighbors that an infected B-node could choose to infect. This effect is represented mathematically by an effective infection probability that is reduced from λ by a factor given by the terms in the parenthesis in Eq. (8). This is depicted in Fig. 3(b) (Region (IV)). There is also an asymmetry in the formation of A-clusters and B-clusters. While one w_1 weighted link in a background of w_0 links leads to the formation of a B-cluster, isolated w_0 links in a background of w_1 links do not lead to A-nodes let alone A-clusters. As a result, $\rho(p)$ is not symmetrical about $p = 1/2$.

For $w < w_c$, the physics is basically the same. The difference is that the smaller contrast w_1/w_0 makes the asymmetry effect in infections between A-clusters and B-clusters less apparent. The inhomogeneous network structure can be considered to be effectively homogeneous with an effective infection probability given by the denominator in the second term in Eq. (6). The smaller contrast makes the effect of the small clusters less important, leading to a mixed phase with finite and non-monotonic ρ over the whole range of p . This is schematically shown in Fig. 3(b) (Region (I)) with the arrows indicating nearly the almost symmetric mutual infections between A-clusters and B-clusters when the contrast is small.

V. QUANTITATIVE TREATMENT

Despite the success of the mean field approach, it only gives a qualitative understanding as much spatial correlation is ignored. Such correlation is important because the chance of infecting a susceptible node depends sensitively on its neighboring nodes and their local environment. A better theory must, therefore, take into account of the local environment of a node. Here, we aim at sketching the key ideas in formulation the theory. For a susceptible node, we label its neighborhood by $S(k, n', n'_I, m'_I)$ when the node is connected to n' neighbors through links of weight w_0 among them n'_I are infected and $k - n'$ neighbors through links of weight w_1 among them m'_I are infected. Similarly, the neighborhood of an infected node can be labelled by $I(k, n, n_I, m_I)$, with the labels in the parentheses taking on the same meaning.

The probability that a susceptible node will be infected depends not only on its neighborhood but also on its infected neighbors' local environment. Figure 5(a) illustrates the different possible combinations that an S node would encounter. An example is given in Fig. 5(b) for $k = 4$, where the S node in the middle has a local environment described by $S(4, 3, 2, 1)$, and its four neighbors are described by $I(4, 1, 0, 1)$ (upper right), $S(4, 3, 1, 1)$ (upper left), $I(4, 2, 1, 0)$ (lower left), and $I(4, 2, 0, 1)$ (lower right). As the system evolves, the numbers of nodes described by $S(k, n', n'_I, m'_I)$ and $I(k, n, n_I, m_I)$ also evolve. These numbers form the variables of the theory. To close the dynamical equations for these variables, we assume a random distribution of neighbors around a node as follows.

Considering an S node of neighborhood $S(k, n', n'_I, m'_I)$,

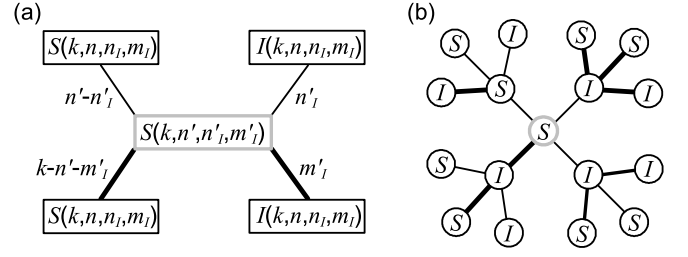


FIG. 5: A better theory is constructed with variables being the local environment of a node. A susceptible node labelled $S(k, n', n'_I, m'_I)$ has n' neighbors connected through links of weight w_0 among them n'_I are infected and $k - n'$ neighbors connected through links of weight w_1 among them m'_I are infected. (a) Schematic diagram showing a susceptible node $S(k, n', n'_I, m'_I)$ connected to neighbors of state S and I and the links could be of weight w_0 (thin lines) or w_1 (thick lines). The neighbor's neighborhood can be labelled accordingly. The probability that the susceptible node is infected in given by $\bar{\lambda}$ in Eq. (18). (b) An example for $k = 4$ in which the susceptible node in the middle has an environment $S(4, 3, 2, 1)$ and its four neighbors have their neighborhood described by $I(4, 1, 0, 1)$, $S(4, 3, 1, 1)$, $I(4, 2, 1, 0)$, and $I(4, 2, 0, 1)$, respectively.

the probability that it is connected to an infected neighbor of neighborhood $I(k, n, n_I, m_I)$ through a link of weight w_0 is assumed to be

$$q_{I,w_0}(k, n, n_I, m_I) = \frac{(n - n_I)f_I(k, n, n_I, m_I)}{\Omega_{I,w_0}}. \quad (12)$$

Here, $f_I(k, n, n_I, m_I)$ is the fraction of nodes in the local environment $I(k, n, n_I, m_I)$ in the system and $\Omega_{I,w_0} = \sum_{n, n_I, m_I} (n - n_I)f_I(k, n, n_I, m_I)$ is a normalization factor. Similarly, the probability that it is connected to an infected neighbor of neighborhood $I(k, n, n_I, m_I)$ through a link of weight w_1 is given by

$$q_{I,w_1}(k, n, n_I, m_I) = \frac{(k - n - m_I)f_I(k, n, n_I, m_I)}{\Omega_{I,w_1}}, \quad (13)$$

where the normalization factor $\Omega_{I,w_1} = \sum_{n, n_I, m_I} (k - n - m_I)f_I(k, n, n_I, m_I)$. Following a similar consideration, the probability that the S node is connected to a susceptible neighbor of neighborhood $S(k, n, n_I, m_I)$ through a link of weight w_0 is given by $q_{S,w_0}(k, n, n_I, m_I) = (n - n_I)f_S(k, n, n_I, m_I)/\Omega_{S,w_0}$. Here, $f_S(k, n, n_I, m_I)$ is the fraction of nodes in the local environment $S(k, n, n_I, m_I)$ in the system and $\Omega_{S,w_0} = \sum_{n, n_I, m_I} (n - n_I)f_S(k, n, n_I, m_I)$. Similarly, we have $q_{S,w_1}(k, n, n_I, m_I) = (k - n - m_I)f_S(k, n, n_I, m_I)/\Omega_{S,w_1}$ for connecting to a susceptible neighbor of environment $S(k, n, n_I, m_I)$ through a link of weight w_1 , with $\Omega_{S,w_1} = \sum_{n, n_I, m_I} (k - n - m_I)f_S(k, n, n_I, m_I)$.

According to Eq. (1), an infected neighbor of neighborhood $I(k, n, n_I, m_I)$ has a probability

$$\mathcal{P}_{w_0}(k, n) = \frac{w_0}{nw_0 + (k - n)w_1} \quad (14)$$

to choose the S node for infection if the link is of weight w_0 , and a probability

$$\mathcal{P}_{w_1}(k, n) = \frac{w_1}{nw_0 + (k-n)w_1} \quad (15)$$

if the link is of weight w_1 . Taking into account of all possible cases of infected neighbors linked through weight w_0 links, the average probability $\bar{\mathcal{P}}_{w_0}$ that the S node is selected for infection through a link of weight w_0 is

$$\bar{\mathcal{P}}_{w_0}(k) = \sum_n \sum_{n_I} \sum_{m_I} q_{I,w_0}(k, n, n_I, m_I) \mathcal{P}_{w_0}(k, n). \quad (16)$$

Similarly, the average probability $\bar{\mathcal{P}}_{w_1}$ the the S node is selected for infection through a link of weight w_1 is

$$\bar{\mathcal{P}}_{w_1}(k) = \sum_n \sum_{n_I} \sum_{m_I} q_{I,w_1}(k, n, n_I, m_I) \mathcal{P}_{w_1}(k, n). \quad (17)$$

Finally, the probability of the S node is infected is given by

$$\bar{\lambda}(k, n', n'_I, m'_I) = 1 - (1 - \lambda \bar{\mathcal{P}}_{w_0}(k))^{n'_I} (1 - \lambda \bar{\mathcal{P}}_{w_1}(k))^{m'_I}, \quad (18)$$

where the second term gives the probability that the node is not infected by any one of the $(n'_I + m'_I)$ infected neighbors via links of either weight w_0 or w_1 .

The dynamical equations of the variables $f_S(k, n, n_I, m_I)$ can now be written down as

$$\begin{aligned} \frac{df_S(k, n, n_I, m_I)}{dt} = & - f_S(k, n, n_I, m_I) \bar{\lambda}(k, n, n_I, m_I) \\ & + f_I(k, n, n_I, m_I) \gamma \\ & + \delta f_S(k, n, n_I, m_I). \end{aligned} \quad (19)$$

The first term in the right-hand-side accounts for the drop in the fraction $f_S(k, n, n_I, m_I)$ when susceptible nodes with neighborhood $S(k, n, n_I, m_I)$ are infected. The second term accounts for the recovery of infected nodes of neighborhood $I(k, n, n_I, m_I)$. When an S node is infected, its neighboring susceptible nodes have a modified neighborhood with one more infected neighbor and the third term accounts for such a change in $f_S(k, n, n_I, m_I)$. As an example, consider the infection of the S node in the middle of Fig. 5(b). In this case, the first term in Eq. (19) accounts for the drop of $1/N$ in the fraction $f_S(4, 3, 2, 1)$ when infection occurs with the probability $\bar{\lambda}$. At the same time, the upper left S node has its neighborhood changed from $S(4, 3, 1, 1)$ to $S(4, 3, 2, 1)$, leading to an increase of $1/N$ given by the third term in Eq. (19) when it is applied to $f_S(4, 3, 2, 1)$.

The dynamical equations of the variables $f_I(k, n, n_I, m_I)$ can also be written down as

$$\begin{aligned} \frac{df_I(k, n, n_I, m_I)}{dt} = & + f_S(k, n, n_I, m_I) \bar{\lambda}(k, n, n_I, m_I) \\ & - f_I(k, n, n_I, m_I) \gamma \\ & + \delta f_I(k, n, n_I, m_I), \end{aligned} \quad (20)$$

with the terms carrying similar meanings as in Eq. (19). Equations (19) and (20) form a closed set of equations for the variables $f_S(k, n, n_I, m_I)$ and $f_I(k, n, n_I, m_I)$. The theory accounts for spatial correlation up to the neighborhoods of the

nearest neighbors of a node. In contrast, the simple mean field approach is a site-approximation that ignores any spatial correlation. Incorporating a longer spatial correlation is often necessary in problems in which the evolution is related to comparing the states of neighboring nodes, as in Refs. [35, 39, 40]. The set of equations can be iterated in time to study the evolution of the systems. Steady state properties can be studied by either setting the equations to zero or iterating the equations to the long time limit. The fraction of infected nodes in the steady state can be found by

$$\rho = \sum_n \sum_{n_I} \sum_{m_I} f_I(k, n, n_I, m_I), \quad (21)$$

which combines the steady state values of $f_I(k, n, n_I, m_I)$ for a random regular network of degree k .

Applying Eqs. (19) and (20) to our model and solving them numerically for different degrees k and infection probabilities gives the results as shown in Fig. 6. The theory agrees reasonable well with simulation data. In particular, the theory is in quantitative agreement with simulation data for both $p \ll 1$ and for a large part of p in which ρ increases. For cases in which ρ goes through a minimum without vanishing, the theory captures the behavior very well, except missing the depth of the minimum. Discrepancies remain, however, in the vicinity where ρ vanishing continuously near p_L and p_R . The theory predicts a range of $p_L \leq p \leq p_R$ with $\rho = 0$, but the values of p_L and p_R are slightly off. The discrepancy shows that the effects of fluctuations in the local environments of S nodes and I nodes near the absorbing transitions are so important that even spatial correlation to the extent that our theory includes is insufficient to capture the behavior near the transitions accurately. Although one could, in principle, include longer spatial correlation by using a bigger set of variables, the theory will involve more complicated and many more equations. The inclusion of spatial correlation up to the neighborhood of nearest neighbors as in the present theory represents a good balance between accuracy and complexity of the theory.

VI. SUMMARY

We proposed and studied in detail the SIS epidemic model with a contact infection process in a network consisting of two different kinds of links mimicking two kinds of relationship. For an infected nodes with k links, a link of heavier weight w_1 has a higher chance of being chosen as the path of infection than a link of weight w_0 . Detailed numerical simulations revealed that the fraction of infected nodes $\rho(p)$ varies with the fraction of w_1 weighted links p non-monotonically. For small contrasts of $w = w_1/w_0$, $\rho(p)$ shows a minimum at a particular value of p that is dependent on the degree k and SIS model parameters. This signifies an optimal suppression of the epidemic. For sufficiently large contrasts, the suppression leads to a range $p_L \leq p \leq p_R$ in which the disease will eventually die off and give rise to a 100% healthy state. This leads to a re-entrance behavior as a function of p , with the system goes through an active epidemic phase, an absorbing healthy phase

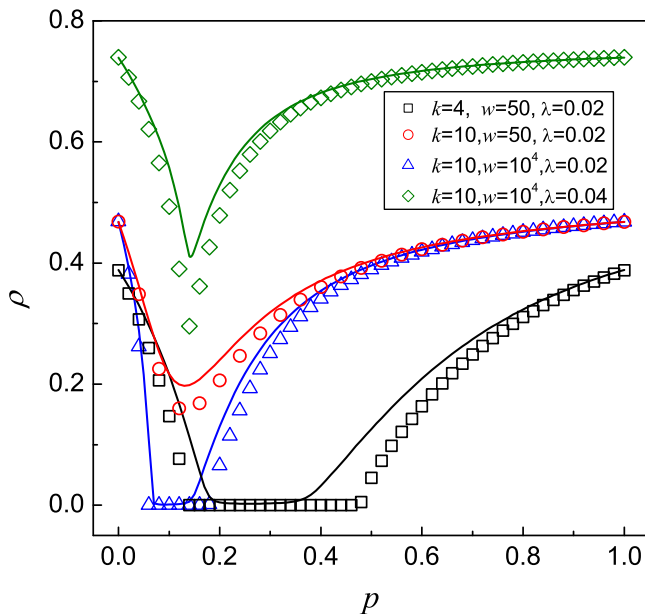


FIG. 6: (color online) The fraction of infected nodes ρ as a function of the fraction p of heavier weighted links as calculated by theory (curves) based on the dynamics of local environment of nodes. Results for different values of k , w and λ are shown. Simulation results (symbols) are included for comparison.

and an active epidemic phase again as p increases. We also studied the effects of different values of k and the infection probability.

Attempts to explain the numerical features proved to be non-trivial. A mean field theory that ignores spatial correlation was formulated. The theory captures all the key features in simulation results, but the agreement is only qualitative. It gives explicit analytic expressions for $\rho(p)$ in the $p \rightarrow 0$ and $p \rightarrow 1$ limits. The limiting values show that the infection probability is effectively reduced in the two limiting cases of having a dilute fraction of w_1 links in a background of w_0 links and vice versa, but the reduction is asymmetric. In addition, it also exhibits the re-entrance behavior when $w > w_c$ and gives an explicit expression for w_c . A merit of the theory is that it leads to a transparent physical picture. The picture emphasizes the importance of clusters formed by nodes with links with the higher weight. These links confine the spread to within a cluster. At small p , the clusters are small and the disease cannot sustain in them. The disease remains only among the nodes with only w_0 links and the infection probability is effectively reduced. At large p , there is a big cluster and infection can be sustained in it. Replacing some w_1 links

by w_0 links reduces the choice of neighbors of the infected nodes and thus effectively reduces the infection probability. For sufficiently large w_1/w_0 , a state of all healthy nodes can be reached for appropriate values of p when the cluster sizes are big enough to disrupt the epidemics via w_0 links and yet they are not big enough for sustaining the epidemics via w_1 in the clusters.

An improved theory that uses the local environment of a node as variables was also formulated. Comparing to the simple mean field theory, it has a large set of variables as a node could be susceptible or infected and it could be connected by k nodes of in either the S or the I state via w_0 or w_1 links. Accounting for the processes that would lead to a change in the number of different local environments, dynamical equations can be constructed for these variables. It was shown that solving the equations in the steady state gives results in good quantitative agreement with simulation results. From the epidemic dynamics, the inclusion of a longer spatial correlation than the single-site mean field theory is necessary. Our work showed that including a biased selection of infection targets in the standard SIS epidemic model leads to a suppressed spread, even to the extent that a healthy state may result. The model studied here can be readily generalized to other types of networks, as well as other types of weight distributions among the links. In the present model, the infection probability λ is taken to be independent of the weight of the link in which the infection takes place. An alternative is to make use of Eq.(1) to drive both the selection of target and infection. Analytically, the quantitative treatment based on the local environment provides a general framework of formulating a reliable theory for other problems where the change in the state of a node is related to its neighborhood and the inclusion of a spatial correlation longer than a single site is unavoidable.

Acknowledgments

One of us (Elvis H.W. Xu) acknowledges the support from a Hong Kong PhD Fellowship awarded by the Research Grants Council of the Hong Kong SAR Government. M. Tang acknowledges the support from the National Natural Science Foundation of China (Grant Nos. 11105025, 91324002). Y. Do acknowledges the support by the Basic Science Research Program through the National Research Foundation of Korea (NRF) funded by the Ministry of Education, Science and Technology (NRF-2013R1A1A2010067). P.M.H. acknowledges the support of a Direct Grant of Research from the Faculty of Science at the Chinese University of Hong Kong in 2013-14.

[1] R. Albert and A.-L. Barabasi, *Rev. Mod. Phys.* **47**, 74 (2002).
 [2] S. N. Dorogovtsev, A. V. Goltsev, and J. F. F. Mendes, *Rev. Mod. Phys.*, **80**, 1275 (2008).
 [3] R. Pastor-Satorras, C. Castellano, P. Van Mieghem, and A.

Vespignani, arXiv:1408.2701v1 (2014).
 [4] C. Castellano, S. Fortunato, and V. Loreto, *Rev. Mod. Phys.* **81**, 591 (2009).
 [5] B. Robert, L. Morabito, and R. D. Christie, *Int. J. Crit. Infras-*

- tract. **4**, 353 (2008).
- [6] E. Bagheri, and A. A. Ghorbani, *Inform. Syst. Front.* **12**, 115 (2009).
- [7] E. Bullmore and O. Sporns, *Nat. Rev. Neurosci.* **10**, 186 (2009).
- [8] M. Kivela, A. Arenas, M. Barthelemy, J. P. Gleeson, Y. Moreno, and M. A. Porter, arXiv:1309.7233v4 (2014).
- [9] J. Gao, S. V. Buldyrev, H. E. Stanley, and S. Havlin, *Nature Phys.* **8**, 40 (2012).
- [10] S. Boccaletti, G. Bianconi, R. Criado, C. I. del Genio, J. Gómez-Gardeñes, M. Romance, I. Sendiña-Nadal, Z. Wang, M. Zanin, *Phys. Rep.* DOI: 10.1016/j.physrep.2014.07.001.
- [11] M. Szell, R. Lambiotte, and S. Thurner, *Proc. Natl. Acad. Sci. USA* **107**, 13636 (2010).
- [12] A. Cardillo, J. Gómez-Gardeñes, M. Zanin, M. Romance, D. Papo, F. del Pozo, and S. Boccaletti, *Emergence of network features from multiplexity.* *Sci. Reps.* **3**, 1344 (2013).
- [13] F. Battiston, V. Nicosia, V. Latora, *Phys. Rev. E* **89**, 032804 (2014).
- [14] V. Nicosia, G. Bianconi, V. Latora, and M. Barthelemy, *Phys. Rev. Lett.* **111**, 058701 (2013).
- [15] J. Y. Kim and K.-I. Goh, *Phys. Rev. Lett.* **111**, 058702 (2013).
- [16] S. V. Buldyrev, R. Parshani, G. Paul, H. E. Stanley, and S. Havlin, *Nature* **464**, 1025 (2010).
- [17] C. S. Gomez, and A. Arenas, *Phys. Rev. Lett.* **111**, 128701 (2013).
- [18] K.-M. Lee, J. Y. Kim, W.-K. Cho, K.-I. Goh, and I.-M. Kim, *New J. Phys.* **14**, 033027 (2012).
- [19] R. Parshani, C. Rozenblat, D. Ietri, C. Ducruet, and S. Havlin, *EPL* **92**, 68002 (2010).
- [20] D. Cellai, E. Lopez, J. Zhou, J. P. Gleeson, and G. Bianconi, *Phys. Rev. E* **88**, 052811 (2013).
- [21] S. Gomez, A. Daz-Guilera, J. Gomez-Gardenes, C. J. Perez-Vicente, Y. Moreno, and A. Arenas, *Phys. Rev. Lett.* **110**, 028701 (2013).
- [22] J. Gomez-Gardenes, I. Reinares, A. Arenas and L. M. Floria, *Sci. Rep.* **2**, 620 (2011).
- [23] W. Wang, M. Tang, H. Yang, Y. Do, Y.-C. Lai, and G.-W. Lee, *Sci. Rep.* **4**, 5097 (2014).
- [24] D. Cai, Z. Shao, X. He, X. Yan, and J. Han, in *Proceedings of the 9th European Conference on Principles and Practice of Knowledge Discovery in Databases*, 2005.
- [25] C.-G. Gu, S.-R. Zou, X.-L. Xu, Y.-Q. Qu, Y.-M. Jiang, D. R. He, H.-K. Liu and T. Zhou, *Phys. Rev. E* **84**, 026101 (2011).
- [26] R. Yang, T. Zhou, Y.-B. Xie, Y.-C. Lai, and B.-H. Wang, *Phys. Rev. E* **78**, 066109 (2008).
- [27] P. Holme and J. Saramaki, *Phys. Rep.* **519**, 97 (2012).
- [28] Z. Yang and T. Zhou, *Phys. Rev. E* **85**, 056106 (2012).
- [29] W. Wang, M. Tang, H.-F. Zhang, H. Gao, Y. Do, and Z.-H. Liu, arXiv:1407.0774v1 (2014).
- [30] Y. Min, X. Jin, Y. Ge, and J. Chang, *PLoS ONE* **8**, e57100 (2013).
- [31] C. Castellano and R. Pastor-Satorras, *Phys. Rev. Lett.* **105**, 218701 (2010).
- [32] M. Boguna, C. Castellano, and R. Pastor-Satorras, *Phys. Rev. Lett.* **111**, 068701 (2013).
- [33] H. K. Lee, P.-S. Shim, and J. D. Noh, *Phys. Rev. E* **87**, 062812 (2013).
- [34] R. Cohen and S. Havlin, *Complex Networks: Structure, Robustness and Function* (Cambridge University Press, Cambridge, 2010).
- [35] P.-A. Noël, B. Davoudi, R. C. Brunham, L. J. Dubé, B. Pourbohloul, *Phys. Rev. E* **79**, 026101 (2009).
- [36] C. Varghese and R. Durrett, *Phys. Rev. E* **87**, 062819 (2013).
- [37] C. Castellano and R. Pastor-Satorras, *Phys. Rev. Lett.* **96**, 038701 (2006).
- [38] M. A. Munoz, R. Juhasz, C. Castellano, and G. Odor, *Phys. Rev. Lett.* **105**, 128701 (2010).
- [39] M. Ji, C. Xu, C. W. Choi, P. M. Hui, *New J. Phys.* **15**, 113024 (2013).
- [40] G. Demirel, F. Vazquez, G. A. Böhme, T. Gross, *Physica D* **267**, 68 (2014).